consideration is given to the orientation dependence of the field on the resonance frequency at the center of the wall and the position dependence of the linewidth in the wall.

One important conclusion to be drawn from our work is that in a ferromagnetic crystal, where the calculated values of η_W/η_D are large, it is unlikely that a domain-rotation-enhancement NMR will be seen in the unsaturated state. This is true irrespective of whether an anisotropic hyperfine interaction exists or not.

ACKNOWLEDGMENTS

The authors gratefully acknowledge important discussions with A. C. Gossard and J. F. Dillion, Jr.

*Research at UCSB supported in part by the National Science Foundation.

†Work performed in part while at the University of California, Santa Barbara, Calif.

[1]I. Tsubokawa, J. Phys. Soc. Japan 15, 1664 (1960).

[2]A. C. Gossard, V. Jaccarino, and J. P. Remeika, Phys. Rev. Letters 7, 122 (1961).

[3]A. C. Gossard, V. Jaccarino, and J. R. Remeika, J. Appl. Phys. 33, 1187S (1962).

[4]H. L. Davis and A. Narath, Phys. Rev. 134, 433 (1964).

[5]C. H. Cobb, V. Jaccarino, J. P. Remeika, R. Silberglitt, and H. Yasuoka, Phys. Rev. B 3, 1677 (1971).

[6]J. F. Dillon, Jr. and M. Teague, Rev. Sci. Instr. 35, 747 (1964).

[7]R. G. Shulman, Phys. Rev. 121, 125 (1961).

[8]An Arenberg Ultrasonic Laboratory PG-650C pulsed oscillator modulated by a General Radio 1395A modular pulse generator formed the incoherent pulses.

[9]A. G. Redfield, Phys. Rev. 98, 1787 (1955).

[10]E. F. Mendis and L. W. Anderson, Phys. Rev. B 2, 569 (1970).

[11]H. Abe, H. Yasuoka, and A. Hirai, J. Phys. Soc. Japan 21, 77 (1966).

[12]I. Solomon, Phys. Rev. 110, 61 (1958).

[13]D. L. Cowan and L. W. Anderson, Phys. Rev. 135, A1046 (1964).

[14]J. F. Dillion, Jr. and J. P. Remeika, J. Appl. Phys. 34, 637 (1963).

[15]A. Abragam, *Principles of Nuclear Magnetism* (Oxford U. P., London, 1961), p. 234.

[16]A. M. Portis and A. C. Gossard, J. Appl. Phys. 31, 2055 (1960).

[17]S. Chikazumi, *Physics of Magnetism* (Wiley, New York, 1964), p. 186.

[18]Y. A. Turov, A. P. Tankeyev, and M. I. Kurkin, Fiz. Metal. i Metalloved. 28, 385 (1969); 29, 747 (1970).

[19]G. A. Murray and W. Marshall, Proc. Phys. Soc. (London) 86, 315 (1965).

[20]H. Suhl, Phys. Rev. 109, 606 (1958); T. Nakamura, Progr. Theoret. Phys. (Kyoto) 20, 542 (1958).

[21]J. M. Winter, Phys. Rev. 124, 452 (1961).

[22]M. B. Stearns, Phys. Rev. 162, 496 (1967).

[23]H. Nagai, T. Hihara, and E. Hirahara, J. Phys. Soc. Japan 29, 622 (1970).

[24]C. H. Cobb and V. Jaccarino, J. Appl. Phys. 42, 1310 (1971).

PHYSICAL REVIEW B VOLUME 7, NUMBER 1 1 JANUARY 1973

Spin Polarization of Electrons Tunneling from Films of Fe, Co, Ni, and Gd†

P. M. Tedrow and R. Meservey

Francis Bitter National Magnet Laboratory, Massachusetts Institute of Technology, Cambridge, Massachusetts 02139

(Received 1 February 1972; revised manuscript received 2 August 1972)

The spin polarization of electrons tunneling from films of Fe, Co, Ni, and Gd to superconducting Al films is determined from conductance measurements. The phenomenological theory of superconducting–normal-metal tunneling is modified to describe superconducting-ferromagnetic tunneling in a magnetic field. The experimental technique and the method of analysis of the conductance curves to obtain the electron polarization are both described. The observed polarization is positive (majority spin direction predominating) for all the metals; the values obtained were Fe, +44%; Co, +34%; Ni, +11%; and Gd, +4.3%.

I. INTRODUCTION

Spin polarization of electrons emerging from ferromagnetic materials has recently been the subject of several investigations. Busch and co-workers[1] have measured the spin polarization of photoelectrons emitted from various ferromagnetic films including Fe, Ni, Co, and Gd. Tedrow and Meservey[2] measured the spin-dependent tunneling between thin films of superconducting Al and ferromagnetic Ni. Gleich and co-workers[3] have studied the spin polarization of field-emitted electrons from different lattice directions of single crystal Ni.

The technique of producing spin-polarized tunneling currents was discovered by Meservey, Ted-

row, and Fulde.[4] It depends on the fact that for very thin superconducting aluminum films, the quasiparticle density of states is split by a magnetic field into spin-up and spin-down parts. The resulting spin densities of states are similar, but displaced from their original energy by $\pm \mu H$, where μ is the magnetic moment of the electron. This displacement allows electrons of either spin direction to be selected from the electrons tunneling from the other electrode, which in the present experiments is a ferromagnetic metal.

On the theoretical side, the electron polarization in ferromagnetic thin films aroused much interest because the sign of the polarization was in each instance positive (that is, in the majority spin direction of the ferromagnet). This result conflicted with theoretical arguments based on band-structure calculations. Attempts to account for the experimental results have been given by Anderson,[5] Wohlfarth,[6] Smith and Traum,[7] Kim,[8] and Politzer and Cutler.[9]

We present here a description of the spin-polarized tunneling method and the results obtained with films of Fe, Co, Ni, and Gd. A short summary of the polarization results has already been published.[10] The tunneling technique measures the spin polarization within 10^{-3} eV of the Fermi energy and complements the photoelectric results at 0.4 and 0.8 eV below the Fermi energy.

II. PHENOMENOLOGICAL THEORY

A. Spin Dependence of Superconductor-Normal-Metal Tunneling

Tunneling between a superconductor and a ferromagnetic metal will be described by slightly modifying the semiphenomenological theory of Giaever and Megerle[11] for tunneling between a superconductor and a normal metal. In the latter case the tunneling current I_{SN} is given by

$$I_{SN} = C_N \int_{-\infty}^{\infty} \rho_S(E)[f(E) - f(E+eV)]\,dE. \tag{1}$$

Here the conductance between the metals when the superconductor is in the normal state is $C_N = (2\pi e/\hbar)\,|M|^2 N_N(0) N_S(0)$, where $|M|$ is the tunneling matrix element, $N_N(E)$ is the density of states of the normal metal, and $N_S(E)$ is the density of states of the superconductor when in the normal state. Both $N_S(E)$ and $N_N(E)$ are assumed to be constant near the Fermi energy. $f = (1+e^{\beta E})^{-1}$ is the Fermi function, where $\beta = 1/kT$. E is the energy in electron volts measured from the Fermi energy of the superconductor, and V is the electric potential of the normal metal with respect to the superconductor. For a BCS[12] superconductor with an energy gap 2Δ the superconducting density of states is $N_S(0)\rho_S$, where ρ_S is

$$\rho_S(E) = \frac{|E|}{(E^2-\Delta^2)^{1/2}}, \qquad |E| \geq \Delta$$

$$\rho_S(E) = 0, \qquad |E| < \Delta. \tag{2}$$

The normalized conductance of the junction σ, that is, the ratio of the conductance at a temperature less than T_c to the conductance in the normal state, is

$$\sigma(V) = \frac{dI_{SN}}{dV}\Big/\frac{dI_{NN}}{dV} = \int_{-\infty}^{\infty} \rho_S(E)\left(\frac{\beta e^{\beta(E+eV)}}{(1+e^{\beta(E+eV)})^2}\right)dE. \tag{3}$$

The second factor in the integrand is a bell-shaped function which is symmetrical about its maximum at $E = -eV$. The magnitude of the maximum is proportional to $1/T$ and at $T = 0$ the function degenerates into a δ function and $\sigma(V)_{T=0} = \rho_S(eV)$. Thus for $T = 0$ the measured conductance is exactly proportional to the superconducting density of states. For a finite temperature well below the superconducting transition temperature, the kernel of the integral is still sharply peaked and the conductance reflects qualitatively the density-of-states function somewhat broadened by the temperature. This situation is illustrated in Fig. 1. The BCS function, ρ_S, is shown in Fig. 1(a). Figure 1(b) represents the second factor in the integrand in Eq. (3) at a finite voltage. The resulting conductance $\sigma(V)$ shown in Fig. 1(c) is the integral over-all energy of the product of the function in Figs. 1(a) and 1(b) as specified by Eq. (3). It should be noted that in this diagram the abscissa is the potential difference measured from the Fermi energy of the superconductor. Since the electronic charge is negative, the electron energy *increases* with *decreasing* V (e being the absolute value of the electronic charge). The validity of this description of tunneling between superconducting and normal metals has been thoroughly demonstrated.[13]

When a high magnetic field is applied to a thin film of a superconductor with very small spin-orbit scattering such as Al, the quasiparticle energies are shifted[4] by $\pm \mu H$, where μ is the absolute value of the magnetic moment of the electron. Figure 2(a) shows how the superconducting density of states is split into spin-up (dotted) and spin-down (dashed) density-of-states curves. For a BCS density of states with no spin-orbit scattering,

$$\rho_S(E) = \rho_\uparrow(E) + \rho_\downarrow(E)$$

$$= \tfrac{1}{2}[\rho_S(E+\mu H) + \rho_S(E-\mu H)], \tag{4}$$

where ρ_S is given by Eq. (2).

When the conductance is calculated for tunneling from such a superconductor into a normal metal we expect that the two spin states will be completely independent and their separate conductances will simply add. Figure 2(b) shows the result of applying Eqs. (3) and (4). The resulting conductance agrees very closely with observed conductance

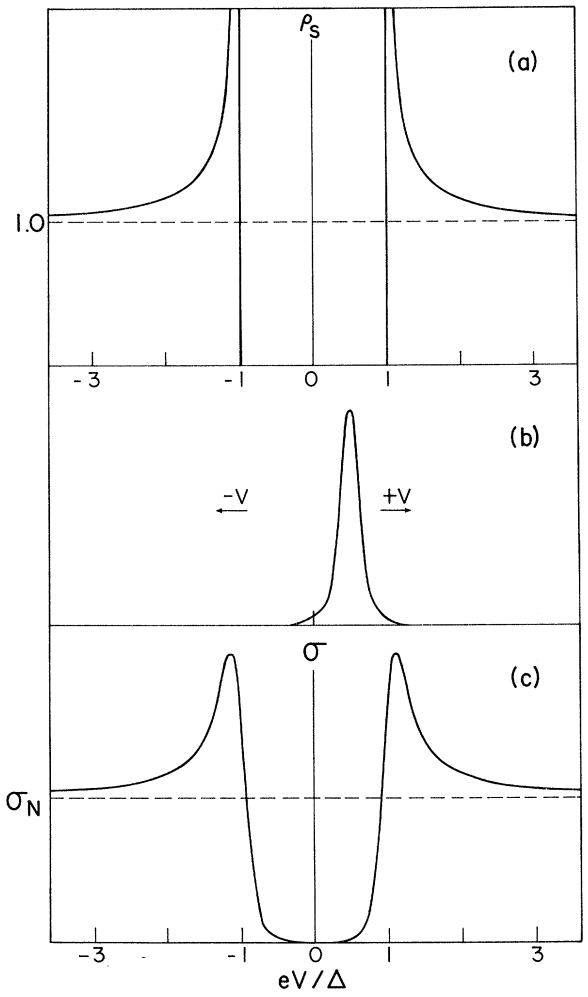

FIG. 1. Superconductor–normal-metal tunneling. (a) BCS density of states of a superconductor as a function of voltage. (b) Temperature-dependent kernel in the integral expression for the conductance. (c) Theoretical normalized conductance σ. Voltage is measured from the Fermi energy of the superconductor. Note that the electron energy decreases as the voltage increases.

curves of an Al-Al_2O_3-Ag junction in a high magnetic field.[4]

B. Superconductor-Ferromagnetic-Metal Tunneling

We wish now to modify the above analysis to apply to tunneling between a superconductor and a ferromagnetic metal. It is assumed that a large magnetic field is applied in the plane of the tunnel barrier so that the magnetization of all domains of the ferromagnetic metal is in the magnetic field direction. In practice, the superconductor is a very thin (≈50-Å) Al film whose plane is also parallel to the field direction so that its critical field is well above the saturation field of the ferromagnetic film.

Most of the assumptions about tunneling from superconductors to normal metals are taken to be valid if the normal metal is ferromagnetic. We assume as before that the spin of the electron is conserved in tunneling. In addition, we assume that the tunneling probability of the two electron-spin states is different, but that the probability for each spin is a constant over the energy region of importance (within about 10^{-3} eV of the Fermi energy). Given these assumptions it is reasonable that the normalized conductance would simply be the sum of the conductances for the two completely independent spin directions. In this case the generalization of Eq. (3) is

$$\sigma(V)=\int_{-\infty}^{\infty} a\rho_S(E+\mu H)\,\frac{\beta e^{\beta(E+eV)}}{(1+e^{\beta(E+eV)})^2}\,dE$$

$$+\int_{-\infty}^{\infty}(1-a)\rho_S(E-\mu H)\frac{\beta e^{\beta(E+eV)}}{(1+e^{\beta(E+eV)})^2}\,dE\ . \quad (5)$$

Here a accounts for the difference in tunneling probability for spin-up and spin-down electrons and is defined as the fraction of tunneling electrons whose magnetic moment is in the direction of the magnetic field (majority electrons in the ferromagnet). That is, $a \equiv n\uparrow/(n\uparrow+n\downarrow)$. The electron polarization is then defined as

$$P\equiv\frac{n\uparrow-n\downarrow}{n\uparrow+n\downarrow}=2a-1\ . \quad (6)$$

Figure 3(a) shows the split density of states of

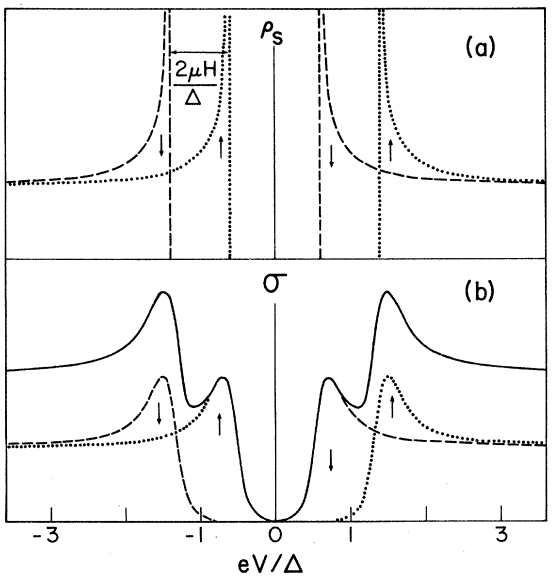

FIG. 2. (a) Magnetic field splitting of the density of quasiparticle states into spin-up (dotted) and spin-down (dashed) densities. (b) Spin-up conductance (dotted), spin-down conductance (dashed), and total conductance (solid line).

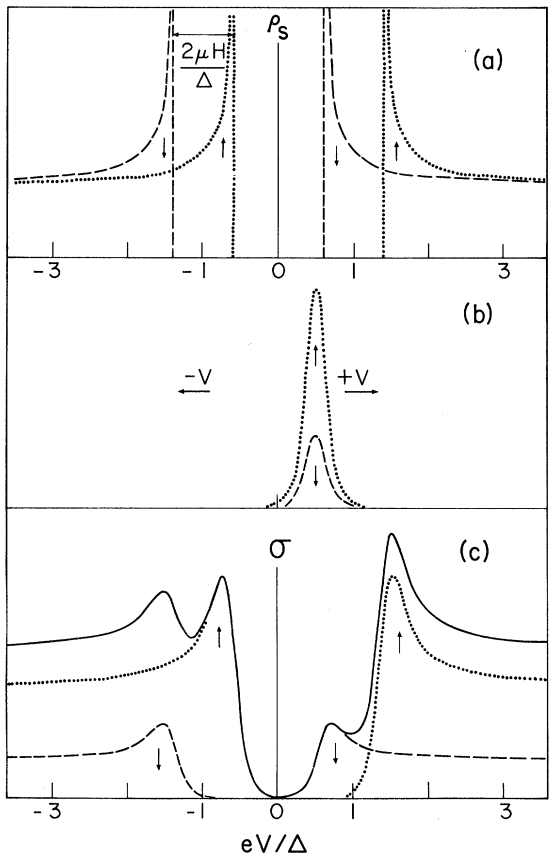

FIG. 3. Superconductor-ferromagnetic metal tunneling. (a) BCS density of states of a superconductor as a function of voltage in a magnetic field. (b) Temperature-dependent kernels for each spin direction in the integral expressions for conductance. (c) Theoretical normalized conductance for each spin direction (dotted and dashed curves) and the total conductance (solid line).

the Al film exactly as in Fig. 2(a). Figure 3(b) shows the second factors in the integrands of Eq. (5) weighted by the factors a and $(1-a)$. For the example shown in Fig. 3, a was chosen to be 0.75, so that $P = 50\%$. Thus for each spin direction there is a sharply peaked function; the functions are similar, only differing by a constant factor which is associated with the relative probability of tunneling in the two spin directions. The resulting conductance is shown as the solid curve of Fig. 3(c). The most striking thing about the conductance function is its asymmetry about $V = 0$. From Fig. 3 we can qualitatively understand the resulting conductance curves. As the voltage is applied to the junction the peaked functions of the ferromagnetic film are moved with respect to the density of states of the Al and reproduce (with some broadening) the corresponding spin density-of-states curve as a conductance curve. Still assuming there is no spin scattering in the tunneling process we should get similar conductance curves for the two spin directions differing by a constant factor $a/(1-a)$ and displaced from each other by an energy of $2\mu H$. The measured conductance in this model is the sum of the conductance curves for the two spin directions.

From the measured conductance curves we can obtain, as explained in Sec. II C, values of the spin polarization P of the tunneling current. The model we have adopted is not explicit as to the physical origin of the polarization of the tunneling currents. As far as this model is concerned it could either be that the density of states of one spin direction is greater in the ferromagnet or that the tunneling matrix element for the two spin directions is different. The main requirement is that, whatever the cause of the differing tunneling conductance in the two spin directions, the tunneling probability is independent of energy over the region in question near the Fermi energy. The assumptions implicit in Eq. (5) are justified by their simplicity and their success in accounting for the measured tunneling conductance. This simple model reproduces the main features of the conductance curves as a function of magnetic field H and yields a value of P independent of H as will be shown in Sec. IV.

C. Analysis of the Conductance Curves (No Spin-Orbit Scattering)

To analyze the conductance curves we first neglect spin-orbit scattering in the aluminum since such scattering has been shown to be small.[14] In addition, we assume there is no spin scattering in the tunneling barrier. This was experimentally shown to be true for Al-Al_2O_3-Al junctions[14] and is expected on theoretical grounds in the high magnetic fields used. As outlined in Sec. II B the conductance curve is taken to be the sum of the conductances for the two spin directions displaced to higher and lower energy by $\pm \mu H$. We assume that the two spin directions have different probabilities (independent of energy) of tunneling into the ferromagnet so the amplitude of the conductance curves in the two spin directions will be different.

Referring to Fig. 3(b), the dashed curve refers to one spin direction, and the dotted curve to the other spin direction. If $f(x)$ is the original unsplit conductance function, we assume that $af(x-h)$ and $(1-a)f(x+h)$ are the conductances of the two spin states. Here a is a constant between 0 and 1, and x and h are measured in electron volts from the Fermi energy of Al; $x = eV$ and $h = -\mu H$ (the negative sign indicating that an increase in voltage corresponds to a decrease in energy of the electron). The solid curve $F(x)$ is the sum of the separate spin conductances, and if the above assumptions are correct, will coincide with the measured curve.

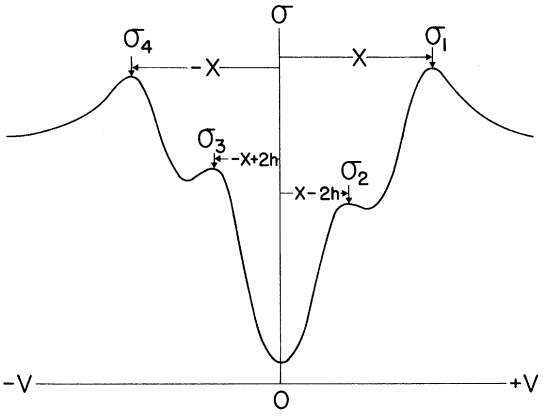

FIG. 4. Values of measured conductance chosen to obtain the polarization from Eq. (9).

It is assumed, in agreement with the BCS theory, that the original function is symmetric about the Fermi surface, that is,

$$f(x)=f(-x)\,. \tag{7}$$

For any value of x we can write four equations for the total (measured) conductance at the points x, $-x$, $x-2h$, and $-x+2h$:

$$\sigma_1=F(x)=af(x-h)+(1-a)f(x+h), \tag{8a}$$

$$\sigma_2=F(x-2h)=(1-a)f(x-h)+af(x-3h), \tag{8b}$$

$$\sigma_3=F(-x+2h)=(1-a)f(x-3h\,af(x-h), \tag{8c}$$

$$\sigma_4=F(-x)=af(x+h)+(1-a)f(x-h). \tag{8d}$$

By elimination we obtain a as a function of the measured conductances σ_1, σ_2, σ_3, and σ_4:

$$a=(\sigma_4-\sigma_2)/(\sigma_4-\sigma_2+\sigma_1-\sigma_3)\,. \tag{9}$$

The polarization as defined by Eq. (6) is $P=2a-1$. From Eqs. (8a) and (8d) we obtain the original function in terms of the quantity a and the measured curve $F(x)$:

$$f(x-h)=\frac{aF(x)-(1-a)F(-x)}{2a-1}\,. \tag{10}$$

Equations (8) imply that any arbitrary value of the voltage x and the magnetic field could be selected to obtain P from Eqs. (8) and (9). In practice, the values of x and h chosen are important in that they determine the accuracy of the result. For very low values of h the fringing field of the incompletely saturated ferromagnetic film acts to change the density of states of Al. This effect will be described later. For values of h very close to the critical field of the Al the depairing of the Al broadens the density-of-states curves and eventually obscures the effect of the magnetic field splitting. Selecting values of x so that σ_1, σ_2, σ_3, and σ_4 are close to the maxima of the conductance curves (or at least in regions where the absolute value of the slope is small) makes the results much less sensitive to random errors. The value of x chosen standardly in calculating P is shown in Fig. 4.

If our assumptions concerning the decomposition of the curves were all correct, Eqs. (9) and (6) would give the polarization and from Eq. (10) we would obtain the conductance function for each spin state at the given applied field. From the conductance the density-of-states function in the Al film could be calculated (at least in theory) by an integral inversion.

D. Effect of Spin-Orbit Scattering

Actually this scheme is no longer exactly valid if there is spin-orbit scattering in the superconductor because in such a case the density of states (and the conductance) of the two spin states is not the same function of the energy. Engler and Fulde[15] have calculated the density of states for various values of spin-orbit scattering. An example of these calculated curves is shown in Fig. 5. It is to be noted that the separate spin densities of states are not symmetrical about the Fermi energy although the total density of states is symmetrical.

To analyze this case we start with two functions, $f_1(x)$ and $f_2(x)$, which for $x\geq 0$ are the conductances of the two spin states corresponding, for example, to the separate densities-of-states curves of Fig. 5. We assume that $f_1(x)$ and $f_2(x)$ (unlike the individual spin densities of states or conductance functions) are symmetric about the Fermi energy, that is,

$$f_1(x)=f_1(-x), \tag{11a}$$

$$f_2(x)=f_2(-x)\,. \tag{11b}$$

From these functions we can construct the total conductance functions above and below the Fermi energy as

$$F(x)=af_1(x)+(1-a)f_2(x)\,,\quad x\geq 0 \tag{12a}$$

$$F(x)=(1-a)f_1(x)+af_2(x)\,,\quad x\leq 0 \tag{12b}$$

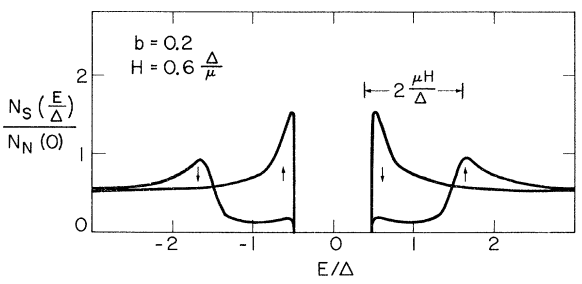

FIG. 5. Spin densities of states calculated by Engler and Fulde for a superconductor with finite spin-orbit scattering.

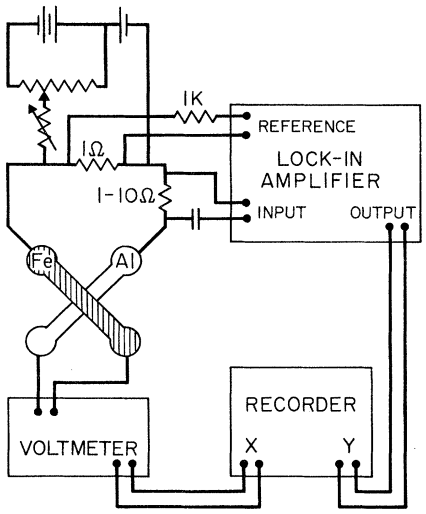

FIG. 6. Schematic circuit diagram for the conductance-vs-voltage measurement.

or from Eqs. (12) we can solve for the unknown functions in terms of the measured total conductance $F(x)$ and the constant a:

$$f_1(x) = \frac{aF(+x) - (1-a)F(-x)}{2a-1} \quad , \tag{13a}$$

$$f_2(x) = \frac{aF(-x) - (1-a)F(+x)}{2a-1} \quad . \tag{13b}$$

$F(+x)$ and $F(-x)$ designate parts of function $F(x)$ for $x \geq 0$ and $x \leq 0$, respectively. Therefore, if we know a or the polarization we can obtain the conductances for the separate spin states. However, we cannot obtain a by simply varying h as before, because the shapes of the functions f_1 and f_2 depend on H and are not simply displaced a distance h. Naturally, if we knew the functional dependence of f_1 and f_2 on H, the value of a would be readily determined. Even though this problem is not yet completely solved, it is important that we can separate the problem into determining the spin density-of-states functions that characterize the superconductor, and the polarization constant P which characterizes the ferromagnetic material used. This separation allows us in principle to employ two different ferromagnetic metals having different values of P with the same superconductor and thereby determine both f_1 and f_2 and the two values of P in a self-consistent manner.

III. EXPERIMENTAL TECHNIQUE

A. Sample Preparation

The tunnel junctions were made in a conventional way. First, an Al film approximately 50 Å thick was evaporated through a mask onto a glass substrate cooled with liquid nitrogen. The pressure during evaporation was about 10^{-5} Torr. The thickness was determined with a quartz-crystal monitor calibrated by multiple-beam interferometer measurements. After evaporation, the Al film was allowed to oxidize for about 4 h in room-temperature air saturated with water vapor. It should be noted that this oxidation procedure when applied to thicker Al films produces thicker oxide layers with very high values of the tunneling resistance. Apparently these very thin Al films oxidize less readily than the thicker films and yield junctions which have a resistance of a few hundred Ω for a 1-mm^2 area at 300 K. After oxidation of the Al, the ferromagnetic metal was evaporated to make a crossed junction. The ferromagnetic films were made 300–1000 Å thick and no effect of the thickness was observed in the measurements. Solder terminals at the ends of the metal strips were evaporated through a third mask. The solder terminals consisted of a 100-Å-thick adherence layer of Cr and a thick layer of indium-tin solder. Copper wires soldered to the terminals gave a four-terminal network.

B. Measurement Technique

The measurements were carried out in the same way as described for Ni in Ref. 2. Figure 6 shows schematically the circuit used to measure the conductance dI/dV as a function of voltage V. The glass slide with the tunnel junction was mounted in a He^3 cryostat so that at low temperatures it was covered with liquid He^3. The temperature was determined by a carbon resistance thermometer calibrated against the helium vapor pressure. The magnetic field was provided by a radial-access Bitter solenoid capable of 60 kOe. The plane of the film was close to vertical and was aligned with the magnetic field by rotating the Dewar. Measurements were made of dI/dV as a function of V at a series of about ten uniformly spaced values of the magnetic field H up to the critical field. Most of the measurements were made at the lowest temperature of the system, about 0.4 K.

IV. MEASUREMENTS

Measurements were made of the tunneling conductance σ as a function of voltage for junctions made of thin Al films and films of Fe, Co, Ni, or Gd. Typical curves for different values of the magnetic field H are shown for Ni, Co, and Fe in Figs. 7–9.

The polarization was calculated by using Eqs. (6), (8), and (9), thereby neglecting the effect of the slight spin-orbit scattering in the Al. The values of polarization will probably be slightly reduced when a correction is made for the small spin-orbit scattering in Al films. Results as a function of field H are shown in Fig. 10. The polarization

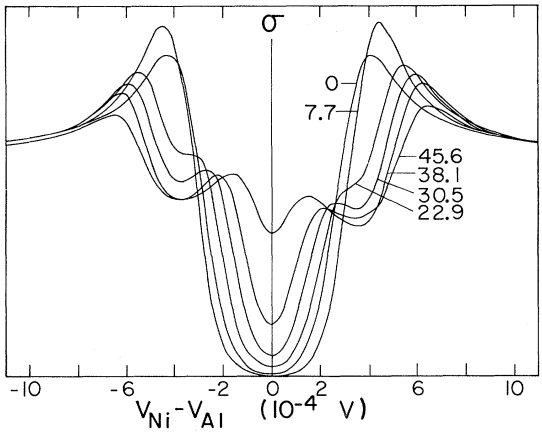

FIG. 7. Measured conductance vs voltage for an Al-Al_2O_3-Ni tunnel junction for several values of the magnetic field H (kOe).

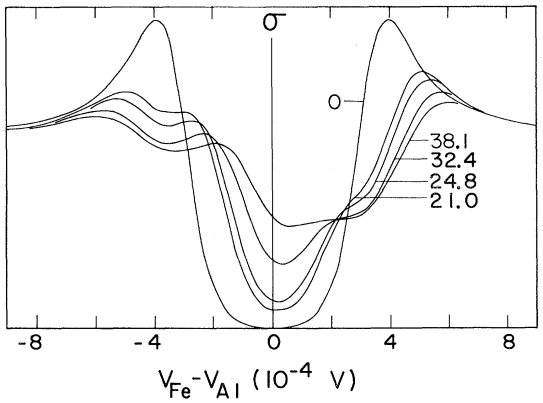

FIG. 9. Measured conductance vs voltage for a typical Al-Al_2O_3-Fe junction at several values of magnetic field H (kOe).

appears to be constant for fields above 15 kOe. This consistency of the polarization for different values of H is perhaps the best evidence for the correctness of the tunneling model leading to Eqs. (8) and (9).

It is probable that at lower fields where the saturation of the ferromagnet is incomplete (and the alignment of domains is incomplete) there is a decrease in the measured polarization. However, at these low fields where the splitting of the spin density of states in the Al was small, the maxima for the two spin states were not resolved and the value of P depended on the details of the rapidly changing conductance curves. At higher fields where the maxima are resolved, the values of σ_1, σ_2, σ_3, and σ_4 near these maxima, as shown in Fig. 4 (at x, $-x$, $x-h$, $-x+h$), are comparatively insensitive to small errors of measurement or analysis. In addition, at fields below saturation the situation becomes more complicated because the fringing fields from the incompletely aligned domains provide a perpendicular field on the Al film (which is only 30 Å away) and cause some depairing. An extreme example of this effect is shown in Fig. 7. The conductance maximum actually increases from $H=0$ to $H=7.7$ kOe before it starts decreasing again because of the combined effect of splitting of the spin states and the depairing because of the parallel magnetic field.

V. DISCUSSION

Table I compares the polarization obtained in the present experiments with the results of the photo-

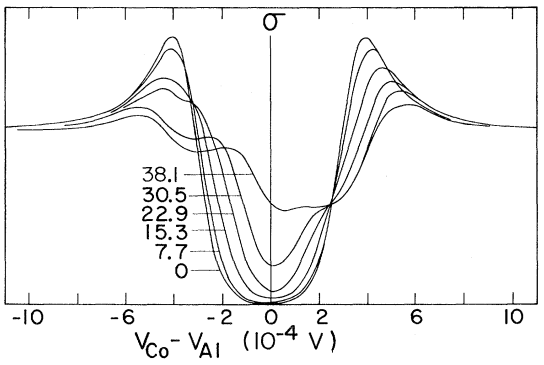

FIG. 8. Measured conductance vs voltage for a typical Al-Al_2O_3-Co junction at several values of magnetic field H (kOe).

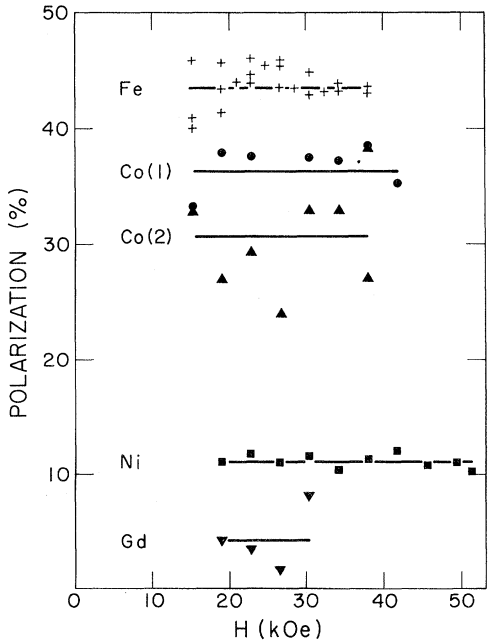

FIG. 10. Apparent electron-spin polarization for four ferromagnetic metals as a function of magnetic field.

TABLE I. Percent polarization P measured in thin ferromagnetic films.

	Tunneling (%)	Photoemission[a](%)
Fe	+44	+54
Co	+34	+21
Ni	+11	+15
Gd	+ 4.3	+ 5.7

[a]These values are the largest obtained with films deposited at room temperature; disordered films deposited at low temperatures had lower values of polarization.

emission experiments. The agreement is generally good. The absolute values of P differ somewhat, but the relative values for films of different ferromagnetic metals are in general agreement, even though the energy region sampled by the measurements is very different. Most striking is the universal positive sign obtained. In the case of Co, the tunneling results have a large spread of measured polarization, even though the random errors for each junction of Co were less than for junctions of Ni and Fe. Co is hexagonal closed packed, whereas Fe and Ni are both cubic. It is possible that there is a lattice directional dependence of the polarization, and different Co films have different amounts of crystal orientation with respect to the glass substrate. A first-order correction for spin-orbit scattering in the Al films indicates that the quoted values of P will probably be reduced when spin-orbit scattering can be allowed for.

Gleich and co-workers[3] have measured the spin polarization of field-emitted electrons from single crystals of nickel. They have observed different values of the polarization in different lattice directions. The values obtained for different directions were -10% [100], -7.8% [110], -9.5% [137], and $+7.5\%$ [111]. The outstanding result is that all directions give a negative polarization except for the [111] direction. On this basis they argue that the thin-film results for Ni are to be explained as a crystal orientation effect with respect to the substrate so that the tunneling and photoemitted electrons are mainly from the [111] direction.

However, there seems to be no independent evidence of such a large degree of crystal orientation in room-temperature deposited Ni films. Even more difficult to explain on this basis are the results of Busch and co-workers[1] on films evaporated at low temperatures where very small crystals are presumably randomly oriented. The values of P are somewhat less but are in each case positive. Gleich and co-workers give $P=-13\%$ for a Ni polycrystalline sample. They also quote a result for Fe as less than 6%. On the basis of these facts it seems probable, but not certain, that the single-crystal results are inconsistent with the thin-film measurements. Further measurements are needed to clarify the experimental picture.

Theoretical explanations of the polarization have not yet been very convincing. Most attempts have been based on calculated properties of the band structure of nickel, which is comparatively well known. There are, however, two empirical generalizations which emerge from the thin-film measurements and which make all explanations based on the details of the band structure of bulk ferromagnetic metals rather suspect. First is the independence of the polarization of the energy levels from which the electrons originate (0.4–0.8 eV below the Fermi energy in the case of the photoemission experiments and $< 10^{-3}$ eV below the Fermi energy in the case of tunneling). Second is the fact that the polarizations are all positive and scale roughly with the magnetic susceptibility of the metal. Both of these facts are difficult to explain by band structure because for the different metals and at different energies one expects the bands to be very different. A possible explanation is that the effective tunneling matrix element depends in some way on the internal magnetic field of the ferromagnet. Although it is not clear how this dependence would arise, such an approach makes the simple correlation of polarization and susceptibility understandable.

ACKNOWLEDGMENTS

We wish to acknowledge many useful discussions with Professor B. B. Schwartz and the help of Richard MacNabb in preparing the tunnel junctions, and Michael Blaho in making the measurements.

†Work supported by the National Science Foundation.

[1]G. Busch, M. Campagna, and H. C. Siegmann, Phys. Rev. 134, 746 (1971); V. Bänninger, G. Busch, M. Campagna, and H. C. Siegmann, Phys. Rev. Letters 25, 585 (1970).

[2]P. M. Tedrow and R. Meservey, Phys. Rev. Letters 26, 192 (1971).

[3]W. Gleich, G. Regenfus, and R. Sizmann, Phys. Rev. Letters 27, 1066 (1971).

[4]R. Meservey, P. M. Tedrow, and P. Fulde, Phys. Rev. Letters 25, 1270 (1970).

[5]P. W. Anderson, Phil, Mag. 24, 203 (1971).

[6]E. P. Wohlfarth, Phys. Letters A36, 131 (1971).

[7]N. V. Smith and M. M. Traum, Phys. Rev. Letters 27, 1388 (1971).

[8]D. J. Kim (unpublished).

[9]B. A. Politzer and P. H. Cutler, Phys. Rev. Letters 28, 1330 (1972).

[10]R. Meservey and P. M. Tedrow, Solid State Commun. 11, 333 (1972).

[11]I. Giaever and K. Megerle, Phys. Rev. 122, 1101 (1961).

[12]J. Bardeen, L. N. Cooper, and J. R. Schrieffer, Phys. Rev. 108, 1175 (1957).
[13]D. H. Douglass, Jr. and L. M. Falicov, in *Progress in Low Temperature Physics*, edited by C. J. Gorter (North-Holland, Amsterdam, 1964), Vol. 4, p. 97.
[14]P. M. Tedrow and R. Meservey, Phys. Rev. Letters 27, 919 (1971).
[15]H. Engler and P. Fulde (unpublished).

PHYSICAL REVIEW B VOLUME 7, NUMBER 1 1 JANUARY 1973

Heat Capacity of Vanadium Oxides at Low Temperature

D. B. McWhan, J. P. Remeika, and J. P. Maita
Bell Laboratories, Murray Hill, New Jersey 07974
and
H. Okinaka, K. Kosuge, and S. Kachi
Department of Chemistry, Faculty of Science, Kyoto University, Kyoto, Japan
(Received 12 July 1972)

The electronic contribution to the heat capacity of $V_{1.97}O_3$, V_7O_{13}, and $V_{0.86}W_{0.14}O_2$ is very large, with $\gamma = (130 \pm 3)$, (80 ± 5), and $(80 \pm 5) \times 10^{-4}$ cal K^{-2}/mole V, respectively. Comparison of effective masses calculated from the heat capacity, magnetic susceptibility, and optical properties suggests that the mass enhancement results mainly from spin fluctuations in a strongly correlated electron gas. The magnetic contribution to the entropy of V_4O_7 at 53 K is 0.32 cal K^{-1}/mole V.

Many temperature-induced metal-insulator transitions occur in oxides of vanadium[1] and titanium.[2] In V_2O_3 the insulating phase is antiferromagnetic (AF),[1] whereas in VO_2 the insulating phase does not order magnetically down to 1.7 K.[3] In the Magneli phases V_nO_{2n-1}, where $3 \leq n \leq 8$, the metal-insulator transitions and the magnetic ordering occur at different temperatures.[4] The available data are summarized in Fig. 1.[5] It is clear that the properties of the oxides containing (a) two *d* electrons per cation (V_2O_3), (b) one *d* electron per cation (VO_2), and (c) a mixture of cations with one or two *d* electrons (V_nO_{2n-1}) are markedly different. By selecting oxides with specific stoichiometries or appropriate transition-metal impurities, it is possible to obtain samples from each of the different classes which are metallic or insulating at low temperatures. Measurement of the heat capacity of these oxides will provide insight into the nature of the metallic states and also some information about the magnetic contributions to the heat capacity and the driving force behind the metal-insulator transitions. In previous studies it was found that the AF insulating phase of V_2O_3 could be suppressed by the addition of Ti_2O_3, and a large linear term in the heat capacity was observed in the metallic phase.[6] The AF phase is also suppressed with excess oxygen,[7] and in the present work the heat capacity of metallic $V_{1.97}O_3$ is compared with that of V_2O_3. V_7O_{13} remains metallic down to 2.5 K (see Fig. 1), and its heat capacity is compared with that of V_4O_7, which is insulating at low temperatures. Finally, the insulating phase of VO_2 can be suppressed by the addition of WO_2, and the heat capacity of metallic $V_{0.86}W_{0.14}O_2$ is compared to that of VO_2. In all cases the metallic phases are found to have greatly enhanced electronic contributions to the heat capacity. Possible origins of this enhancement and their relationship to the metal-insulator transitions are discussed. The magnetic entropy of V_4O_7 is related to the crystal structure of the insulating phase.

I. SAMPLE PREPARATION

$V_{1.97}O_3$

A single crystal was grown by the vapor-transport method using $TeCl_4$[8] and a powder sample of $V_{1.97}O_3$. The powder sample was made by heating the appropriate mixture of V_2O_3 and V_2O_5 in an evacuated quartz tube at 600 °C for three days and then at 1000 °C for seven days. A Guinier x-ray powder pattern taken on crushed crystals showed the corundum structure with $a = 4.948(1)$ Å and $c = 13.989(2)$ Å. X-ray measurements were made relative to a Si internal standard at 4.2 K using a Philips diffractometer and an Air Products Cryotip attachment. The lattice parameters at 4.2 K are $a = 4.932(1)$ Å and $c = 14.002(3)$ Å. As in previous studies on pure and doped metallic V_2O_3, the *c* axis contracts on warming.[9] This probably reflects an expansion of the V-V interatomic distance with decreasing c/a ratio as in the case of Cr-doped V_2O_3.[10] The electrical resistivity was found to decrease smoothly with decreasing temperature with $\rho_{298} \sim 2 \times 10^{-3}$ Ω cm and $\rho_{298}/\rho_{4.2} \sim 3$. No anomalous rise in re-